Isolation, Characterization and Electron Microscopic Single Particle Analysis of the NADH:Ubiquinone Oxidoreductase (Complex I) from the Hyperthermophilic Eubacterium *Aquifex aeolicus*†

Guohong Peng,‡,§ Günter Fritzsch,‡ Volker Zickermann,|| Hermann Schägger,|| Reinhardt Mentele,⊥ Friedrich Lottspeich,⊥ Mihnea Bostina,‡ Michael Radermacher,‡ Robert Huber,# Karl Otto Stetter,# and Hartmut Michel*,‡

Max-Planck-Institut für Biophysik, Frankfurt a. M., Germany, Institute of Oceanology, Chinese Academy of Sciences, Qingdao, China, Gustav-Embden Zentrum der Biologischen Chemie, Klinikum der Johann Wolfgang Goethe-Universität, Frankfurt a. M., Germany, Max-Planck-Institut für Biochemie, Martinsried, Germany, and Universität Regensburg, Lehrstuhl für Mikrobiologie & Archaeenzentrum, Regensburg, Germany

Received September 20, 2002; Revised Manuscript Received January 6, 2003

ABSTRACT: The proton-translocating NADH:ubiquinone oxidoreductase (complex I) has been purified from *Aquifex aeolicus*, a hyperthermophilic eubacterium of known genome sequence. The purified detergent solubilized enzyme is highly active above 50 °C. The specific activity for electron transfer from NADH to decylubiquinone is 29 U/mg at 80 °C. The *A. aeolicus* complex I is completely sensitive to rotenone and 2-*n*-decyl-quinazoline-4-yl-amine. SDS polyacrylamide gel electrophoresis shows that it may contain up to 14 subunits. N-terminal amino acid sequencing of the bands indicates the presence of a stable subcomplex, which is composed of subunits E, F, and G. The isolated complex is highly stable and active in a temperature range from 50 to 90 °C, with a half-life of about 10 h at 80 °C. The activity shows a linear Arrhenius plot at 50−85 °C with an activation energy at 31.92 J/mol K. Single particle electron microscopy shows that the *A. aeolicus* complex I has the typical L-shape. However, visual inspection of averaged images reveals many more details in the external arm of the complex than has been observed for complex I from other sources. In addition, the angle (90°) between the cytoplasmic peripheral arm and the membrane intrinsic arm of the complex appears to be invariant.

The proton pumping NADH:ubiquinone oxidoreductase (complex I) is the first energy transducing complex of the respiratory chain. It couples the transfer of electrons from NADH to ubiquinone to the generation of an electrochemical proton gradient across the membrane that drives energy consuming processes such as ATP synthesis and flagella movement (*1*−*4*). Complex I is the most complicated and least understood multisubunit enzyme in the respiratory chain of mitochondria and aerobic bacteria (*5*, *6*). So far, complex I has been isolated from eukaryotic mitochondrial membranes, from chloroplasts of plants, and from prokaryotic cytoplasmic membranes (*7*−*10*). The bacterial complex I has a molecular mass of about 550 kDa. In *Eschericha coli*, 14 genes are organized in one operon specifying its minimal structure (*11*). The mitochondrial complex I is even larger, with a molecular mass of around 1 mDa, and comprises at least 43 subunits. Electron microscopy and single particle analysis shows that the complexes are L-shaped, with a peripheral arm and a membrane intrinsic arm of nearly equal length (*12*−*14*). Complex I isolated from several bacteria appears to be both unstable and of varying morphology (*7*). The *E. coli* complex I is the only bacterial enzyme being isolated so far in an intact form (*6*, *15*). The reasons for the difficulties in obtaining a homogeneous complex I from bacteria, yeast, or mammals are revealed by electron microscopy, where each preparation shows particles of varying shapes. This finding may explain why no crystals of complex I have been reported yet, and no high resolution structure of the enzyme has been determined. In addition, until stable and homogeneous preparations are obtained, the structure and catalytic mechanism of the enzyme will be discussed controversially (*16*−*18*).

Hyperthermophilic microorganisms are a diverse group adapted to growth temperatures above 80 °C (*19*). The enzymes of these organisms are attractive for studies of structural and functional adaptation to high temperature and for biotechnological applications because they are stable and active even under conditions that were previously regarded as incompatible with life. *A. aeolicus* is a microaerophilic, obligate chemolithoautotrophic eubacterium, with a maximum growth at about 95 °C (*20*). It is the first hyperthermophilic eubacterium with a completely sequenced genome (*20*, *21*). In contrast to other organisms, genes encoding the enzyme for many metabolic pathways are not functionally

† This work was supported by the Max-Planck-Society, the Fonds der Chemischen Industrie, and in part by Chinese Academy of Sciences.

* To whom correspondence should be addressed. Tel.: 49-69-96769-401. Fax: 49-69-96769-423. E-mail: Hartmut.Michel@mpibp-frankfurt.mpg.de.

‡ Max-Planck-Institut für Biophysik.

§ Chinese Academy of Sciences.

|| Klinikum der Johann Wolfgang Goethe Universität.

⊥ Max-Planck-Institut für Biochemie.

Universität Regensburg.

10.1021/bi026876v CCC: $25.00
Published on Web 02/20/2003

grouped in operons in *A. aeolicus*, instead, they are dispersed throughout the genome. This feature is even found for the genes encoding the subunits of protein complexes. Genes encoding potential subunits of complex I are located in three different operons, and for many of these subunits two or three homologous genes are found (*21*, *22*). Given the ecological niche occupied by *A. aeolicus* and the apparent genetic complexity of complex I, we have set out to investigate the properties of this multisubunit complex. Some properties of this enzyme in membranes of *A. aeolicus* have been reported (*23*). Here, we describe the first purification of a highly stable and active complex I from this hyperthermophilic eubacterium and its further characterization. Electron microscopy and single particle analysis reveals a complex having the typical L-shape. Visual inspection of averaged images reveals clearer details in the cytoplasmic domain of the complex, and an invariant angle (90°) between the base domain of the cytoplasmic arm and the membrane arm as compared with complex I preparations from other species, indicating a better preservation of the enzyme and a more homogeneous preparation.

MATERIALS AND METHODS

Purification of Complex I. A. aeolicus cells were stored at −20 °C, and 40 g batches of thawed cells were resuspended in 200 mL of buffer containing 50 mM Tris-HCl (pH 7.4) and disrupted using a microfluidizer (Model: 110 LA, Microfluidics Corporation, New, Massachusetts) at 1000 MPa. Cell debris was removed by centrifugation at 10 000 *g* for 15 min, and membranes were sedimented from the supernatant by centrifugation at 100 000 *g* for 1 h. The membranes were washed and resuspended in the same buffer at an approximate protein concentration of 12 mg/mL and stored in aliquots at −80 °C.

Dodecyl-β-D-maltoside (GLYCON, Luckenwalde, Germany) was added to the membrane suspension to a final concentration of 3% (w/v), and the suspension was slowly stirred at 40 °C for 1 h. The detergent treated membranes were centrifuged at 100 000 *g* for 1 h to remove nonsolubilized material. The supernatant was loaded onto a Mono Q HR 10/10 column (Pharmacia Biotech), preequilibrated with five column volumes of 20 mM Tris-HCl buffer (pH 7.4), 0.05% sodium azide, and 0.05% dodecyl-β-D-maltoside. The bound proteins were eluted with a linear gradient of 0−0.5 M NaCl, pH 7.4. The fractions showing complex I activity were collected and then concentrated to approximately 5 mg/mL using 10 kDa cutoff centriprep filters (Amicon, Beverl, MA) and then loaded onto a TSK 4000 (Tosoh, Japan) or Superdex 200 (Pharmacia) gel filtration column. The columns were eluted with 20 mM Tris-HCl buffer (pH 7.4), 150 mM NaCl, 0.05% sodium azide, and 0.05% dodecyl-β-D-maltoside. Protein samples were stored at −80 °C.

Gel Electrophoresis and Sequencing of the Protein. The sample was subjected to analytical isoelectric focusing (IEF)[1]. Servalyt 3-10 was used. IEF was performed according to the manufacturer's instructions (Servalyt precotes, Serva) with the following modifications: The gel was preincubated with 2% (v/v) Servalyt, 5% (v/v) of glycerol, and 0.05% (w/v) dodecyl-β-D-maltoside for 30 min, and dried at room temperature for 1 h.

The polypeptide composition of the complex I was determined by SDS polyacrylamide gel electrophoresis (PAGE) using a 5−20% linear polyacrylamide gradient or 15% polyacrylamide (*24*). The protein sample was boiled for 3 min in sample buffer. Gel electrophoresis was performed at 4 °C, and the protein bands were visualized by Coomassie blue R250 or silver staining. Protein concentrations were measured by the Microtiter Plate BCA Assay (Pierce). For sequencing, the proteins were transferred onto a PVDF membrane using a semi-dry blotting apparatus by applying 1.5 mA/cm^2 gel for 1.5 h at 4 °C. After transfer, the membrane was stained and destained according to ref *25*, and the proteins were then ready for N-terminal sequencing and mass spectrometric analysis.

Enzyme Activity Assay. The activity of complex I was assayed by monitoring electron transfer from NADH to the ubiquinone analogue 6-decyl-ubiquinone (DQ, 80 μM) as electron acceptor. The assay buffer was prepared as described (*26*). Samples were diluted to 12−15 μg/mL (membranes) and 1−3 μg/mL (complex I). A total of 2.5 μM rotenone was added as a specific inhibitor where indicated. The reaction was started by adding 150 μM NADH to the solutions of the sample premixed in the cuvette with DQ, with or without inhibitor. The time course of NADH oxidation was monitored over 5 min at 80 °C, using a UV−VIS spectrophotometer (DW 2000, SLM AMINCO) equipped with a rapid mixing apparatus. The absorption difference of $\lambda = 340$ nm minus $\lambda = 400$ nm was measured.

Electron Microscopy and Image Analysis of Negatively Stained Complex I. Complex I (6 μL, 0.07 mg/mL of protein) purified by anion exchange plus TSK 4000 and Superdex 200 chromatography was applied to 400 mesh copper grids coated with a thin carbon film. The specimen was stained with 2% ammonium molybdate using a deep staining technique based on the method developed by Stoops et al. (*27*). Micrographs were recorded under low dose conditions on a Philips CM120 electron microscope (FEI, Holland) equipped with a LaB_6 cathode at an accelerating voltage of 100 kV and a calibrated magnification of 58 300×. Selected micrographs were scanned on a Zeiss SCAI flat bed scanner (Zeiss, Germany) with 7 μm raster size. Images were converted to SPIDER format and reduced three times by binning to a final pixel size corresponding to 0.36 nm on the sample scale. Image processing was carried out using SPIDER (version 5.0 modified), WEB (*28*), and XMIPP (*29*).

For image analysis, 1500 particles were picked from eight micrographs selecting those that were separated from neighboring particles and excluding obvious fragments. These images were normalized with the average background of the micrograph. All alignments were performed using a simultaneous translational/rotational alignment algorithm, based on the correlation of Radon transforms (*30*). A preliminary alignment was made using an L-shaped image as reference and its mirror image and applied to 380 particles. Two averages were obtained, which then were used for the alignment of all 1500 images. The aligned images were analyzed with a neural network algorithm (*31*) using an array of 7 × 7 nodes. Two nodes corresponding to a flip and flop orientation of the molecules were used as references for a

[1] Abbreviations: IEF, isoelectric focusing; PAGE, polyacrylamide gel electrophoresis; DQ, 6-decyl-ubiquinone; DQA, 2-*n*-decyl-quinazoline-4-yl-amine.

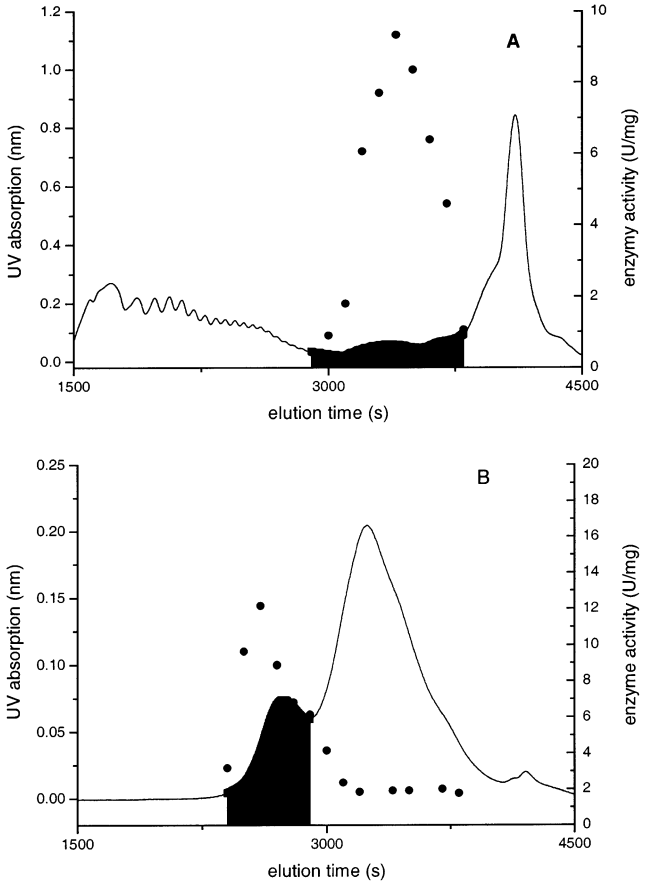

FIGURE 1: Isolation of *A. aeolicus* complex I. (A) Chromatography on a Mono Q ion exchange column; (B) gel filtration on a TSK 4000 column; (−) absorbance at 280 nm; and (●) NADH/decylubiquinone oxidoreductase activity.

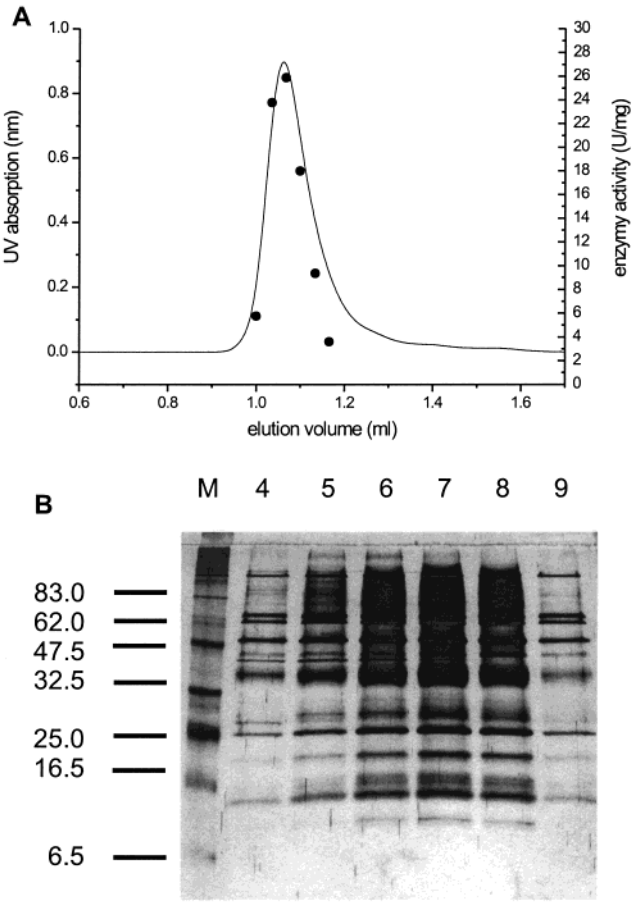

FIGURE 2: Homogeneity of *A. aeolicus* complex I determined by SDS−PAGE. (A) Additional gel filtration chromatography using superdex 200 column; (−) absorption at 280 nm; and (●) enzyme activity. (B) SDS−PAGE (15% polyacrylamide gel) of the fractions of superdex 200 with NADH/decylubiquinone reduction activity (fractions 4−9) visualized by silver staining. The numbers on the left refer to the apparent molecular masses of marker proteins (in kDa).

multireference alignment, and the data set was split into two classes. The alignment was repeated three times, each time using the two class averages as new references. The microscope transfer function was determined for each micrograph, and the originally picked images were corrected for defocus and astigmatism by phase flipping. These corrected images then were again aligned to the last two references by multireference alignment. Finally, two averages were obtained corresponding to the flip and flop related positions of the particles on the carbon film, comprising 815 and 685 particles, respectively.

The resolution for each class average was determined by Fourier ring correlation (*32*) using a cut off criterion of five times the noise correlation. The resolution was estimated to be 2.6 nm before correcting for the microscope transfer function and between 2.1 and 2.2 nm after correction.

RESULTS

Purification of Complex I. Complex I was isolated from *A. aeolicus* membranes solubilized with dodecyl-β-D-maltoside followed by anion exchange chromatography and TSK 4000 gel filtration (Figure 1A,B). It was first eluted from a Mono Q column with a salt concentration gradient of 100−150 mM NaCl at pH 7.4 (Figure 1A). Fractions with complex I activity were collected and most of the other proteins were already removed at this step. The protein was further purified on a TSK 4000 gel filtration column (Figure 1B). The first peak was enriched in complex I. Using yeast cytochrome−bc1 complex dimers with two bound Fv fragments as a standard (molecular mass: 505.5 kDa, ref *33*), the molecular mass of complex I on the Superdex 200 column (Pharmacia, Biotech) was found to be greater than 520 kDa. Figure 2 shows the activity profile (A) and the protein bands analyzed by SDS−PAGE (B) when the purified complex I was rerun on a superdex 200 column. Each fraction shows nearly identical subunit composition on SDS−PAGE.

Table 1: Yield and Purity of Complex I

preparation	protein (mg)	specific activity (U/mg)	total units (U)	yield (%)
membranes	(81.75)[a]	(0.132)	10.8	100
solubilized protein	126.6	0.015	1.9	17.75
Mono-Q	2.96	0.606	1.8	16.75
TSK4000	0.05	19.3	0.97	8.98

[a] The amount of protein was determined using the BCA assay. We find that this assay yields unrealistically low values when unsolubilized membranes are used.

Representative data for complex I purification are listed in Table 1. Dodecyl-β-D-maltoside solubilized the membranes, with an apparent loss of 80% of complex I activity. It is a very common observation that complex I loses quinone reduction ability upon solubilization and purification (*7*−

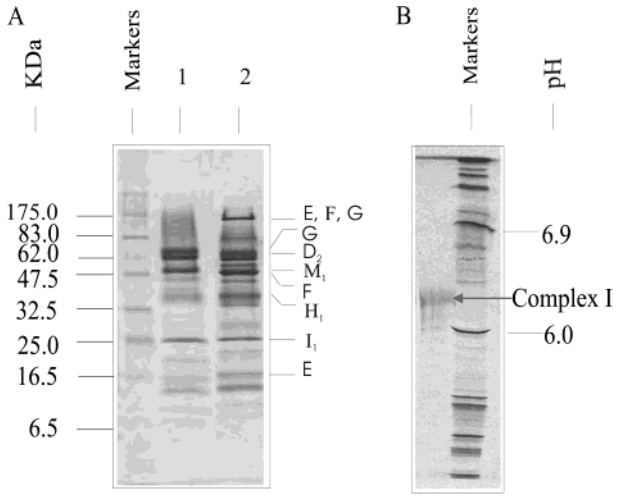

FIGURE 3: SDS−PAGE after incubating the sample at different temperatures and analytical isoelectric focusing. (A) SDS−PAGE (5−20% polyacrylamide gradient gel) of *A. aeolicus* complex I visualized by Coomassie staining. The numbers refer to the molecular masses of markers (in kDa). Lane 1: sample boiled for 3 min. Lane 2: sample incubated at 80 °C for 3 min. Subunits that could be N-terminally sequenced are on the right. (B) Isoelectric focusing in pH range from 3 to 10; the isoelectric points of two standard proteins are indicated.

9). However, it is likely that the access of quinone to its binding site may be different for the membrane embedded complex as compared to the detergent solubilized one, so that the assay conditions are not comparable. The enzyme activity was almost completely retained during the anion exchange chromatography, but there was a 50% loss of activity during TSK 4000 gel filtration. Both steps retain substantial amounts of protein and together provide a more than 1000-fold increase in specific activity over the initially solubilized membrane. The specific activity of the preparation after TSK 4000 gel filtration, measured as rotenone-sensitive electron transfer from NADH to DQ, was 19.3 U/mg, with a final yield of 9%.

Subunit Composition of Complex I. Figure 3A shows the subunit composition of the purified complex I. At least 14 bands were resolved by silver and Coommasie stained SDS−PAGE when the sample was boiled (Figure 3A, lane 1). Figure 3A, lane 2, shows the band pattern when the sample was not boiled but only heated at 40 °C. Apparently, some of the bands did not originate from individual subunits but were formed by aggregates or more likely by sample buffer resistant subcomplexes. The sequencing results show that the subcomplex consists of subunits E, F, and G. The temperature dependence of the band pattern of complex I showed that the subcomplex was stable at 40−80 °C. This result may indicate that the three subunits form one highly stable structural subcomplex in complex I. Seven protein subunits were identified by N-terminal sequencing and mass spectrometry; these are nuo D_2, nuo E, nuo F, nuo G, nuo H_1, nuo I_1, and nuo M_1 (Table 2). Using the web tool TMHMM 2.0 (*34*, *35*), subunits H_1 and M_1 are predicted to have eight and 14 transmembrane spanning segments, respectively. The total number of membrane spanning segments in complex I of *A. aeolicus* is estimated to be at least 63. Complex I focused as a single broad band with an isoelectric point of 6.2 as determined by analytical scale IEF as compared with standards (Serva, Test mixture for PI determination) on a pH 3−10 Servalyt system (Figure 3B).

Table 2: Predicted Complex I Subunits of *A. aeolicus*[a]

subunit	molecular mass (kDa)	N-terminal sequences as determined by protein sequencing	no. of predicted membrane spanning segments
Nuo A_1	14.83		3
Nuo A_2	13.33		3
Nuo B	19.88		0
Nuo D_1	68.69		1
Nuo D_2*	67.89	MKWVNKGTVER	0
Nuo E*	18.55	MFKTEFEFPEE	0
Nuo F*	47.51	MRSYPAIPRYIYAE	0
Nuo G*	72.78	SEKVKIYIDD	0
Nuo H_1*	36.92	MEATAYS	
Nuo H_2	28.79		8
Nuo H_3	11.60		5
Nuo I_1*	23.41	GVKKLSRKDYLNI	3
Nuo I_2	24.57		0
Nuo J_1	17.86		0
Nuo J_2	19.38		5
Nuo K_1	10.74		5
Nuo K_2	10.90		3
Nuo L_1	68.94		3
Nuo L_2	88.99		16
Nuo L_3	71.95		20
Nuo M_1*	55.03	METLLNVA	16
Nuo M_2	56.53		14
Nuo N_1	51.29		14
Nuo N_2	54.27		14
			14

[a] The membrane spanning segments were predicted using the TMHMM server, v. 2.0 (*32*, *33*). The subunits identified by protein sequencing are marked with an asterisk.

Catalytic Activity and Stability. The specific activity of the purified *A. aeolicus* complex I was measured in the temperature range from 50 to 85 °C. The rotenone sensitive activity of complex I increases essentially linearly from 50 to 85 °C. The substrate for the assay was stable in this range of temperature, with no detectable oxidation or degradation of NADH. An Arrhenius plot is shown in Figure 4 and yields an activation energy of 31.92 J/mol K (line a). In addition, the membrane bound enzyme shows a higher activation energy than the isolated enzyme and yields 69.5 J/mol K (line b). The difference might be caused by different access of substrates in the membrane integrated complex as compared to the solubilized complex I.

The high stability of the enzyme is indicated by retention of 80% of its activity during incubation at 80 °C for 8 h (Figure 5). After this time, the activity decreased more rapidly, and 50% of the activity was lost after 10 h. Exposure of the enzyme to pH values in the range of 4.5−9 for 1 h showed no dissociation of the complex that could have been detected by size-exclusion chromatography. Whereas exposure to pH 4.5 had no effect on the activity of the enzyme, exposure to pH 9.0 caused a loss in activity of about 50%. It seems that the complex is sensitive to basic conditions.

The results of inhibitor studies are shown in Figure 6. Both rotenone and DQA inhibit the activity of complex I, with DQA showing higher affinity. The relative IC_{50} values are approximately 0.4 and 2 μM for DQA and rotenone, respectively.

Electron Microscopy of the Negatively Stained Particles and Image Processing. The purified complex I was analyzed by electron microscopy and image processing. L-shaped particles are clearly visible in the electron micrograph (Figure

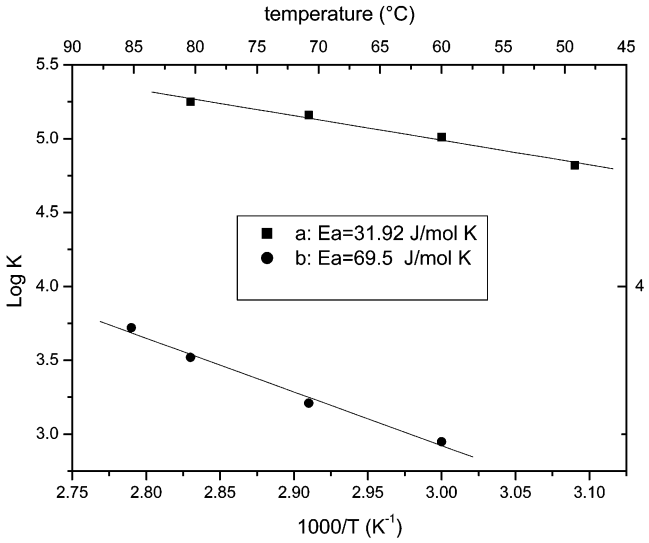

FIGURE 4: Arrhenius plot of *A. aeolicus* complex I. The NADH/decylubiquinone activity was determined as described in the Materials and Methods at temperatures ranging from 50 to 85 °C. Isolated enzyme (0.25 mg/mL) as incubated at 50, 60, 70, and 80 °C, respectively; membrane bound enzyme (6 mg/mL) as incubated at 60, 70, 80, and 85 °C; (a) purified enzyme; and (b) membrane bound enzyme.

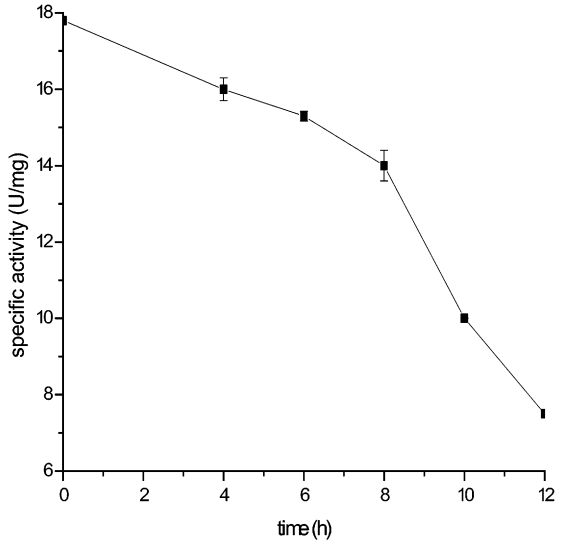

FIGURE 5: Time dependence of the activity of the *A. aeolicus* complex I (a small fraction with the highest activity after Mono Q chromatography was used) when incubated at 80 °C. Data points are the averages of three experiments. Error bars represent standard errors of the mean.

7) of a negatively stained complex I preparation. A neural network analysis of 1500 aligned particles (Figure 8A) showed as the main difference two groups of images, corresponding to the flip/flop related positions of the particles on the grid. Two-dimensional averages of both classes (Figure 8B,C) show a horizontal arm of about 20 nm in length and 5.5 nm in width. The vertical arm can be divided into two domains: a base (B) and a peripheral domain (P). Between the base and the peripheral domain a low density gap (G) can be observed. Within the peripheral domain there is a further low density area with a diameter of about 1.8 nm. The resolution of both averages was estimated to be approximately 2.2 nm (Figure 9), determined by the Fourier ring correlation with a cut-off level of five times the noise correlation. Another significant morphologic characteristic

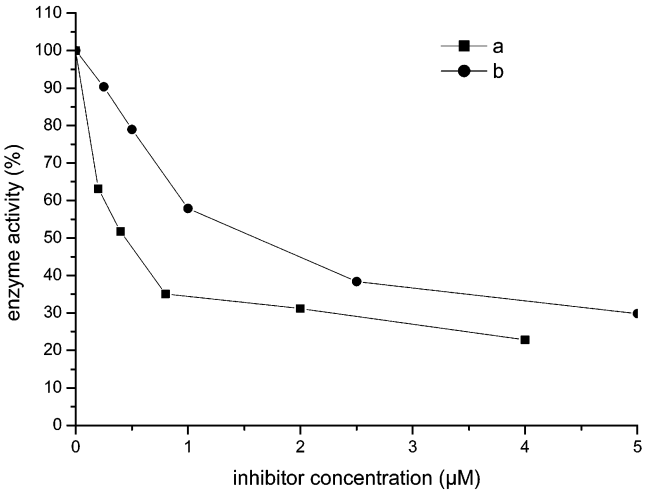

FIGURE 6: Effects of DQA and rotenone on the activity of *A. aeolicus* complex I at 80 °C. Data points are the averages of three experiments. (a) Effects of rotenone; and (b) effects of DQA.

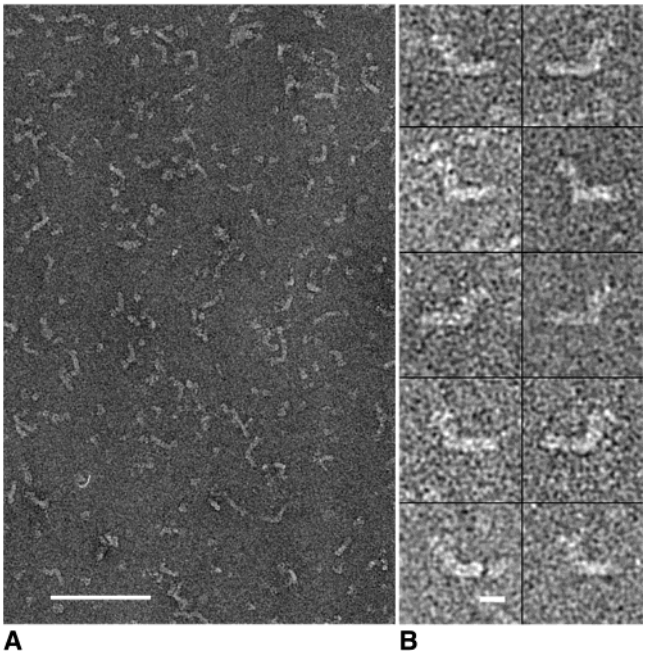

FIGURE 7: (A) Electron micrographs of *A. aeolicus* complex I particles in deep stain (scale bar 100 nm). (B) A gallery of particles, selected for image processing (scale bar 10 nm).

is that the base domain in the vertical arm is always connected by an angle of 90° to the horizontal arm.

DISCUSSION

Complex I is the largest and the most complicated enzyme in the respiratory chains of bacteria and mitochondria. Unlike other major components of the chain, no high resolution structural data have been obtained so far (*36*, *18*). This fact greatly hampers the design of directed experiments to a detailed understanding of the mechanism of action of this important enzyme. A common explanation for this deficit is the difficulty in obtaining stable, homogeneous, detergent-solubilized preparations of this large membrane protein complex with high catalytic activity and inhibitor sensitivity (*37*, *38*).

This report describes the purification and first characterization of the proton pumping NADH:ubiquinone oxi-

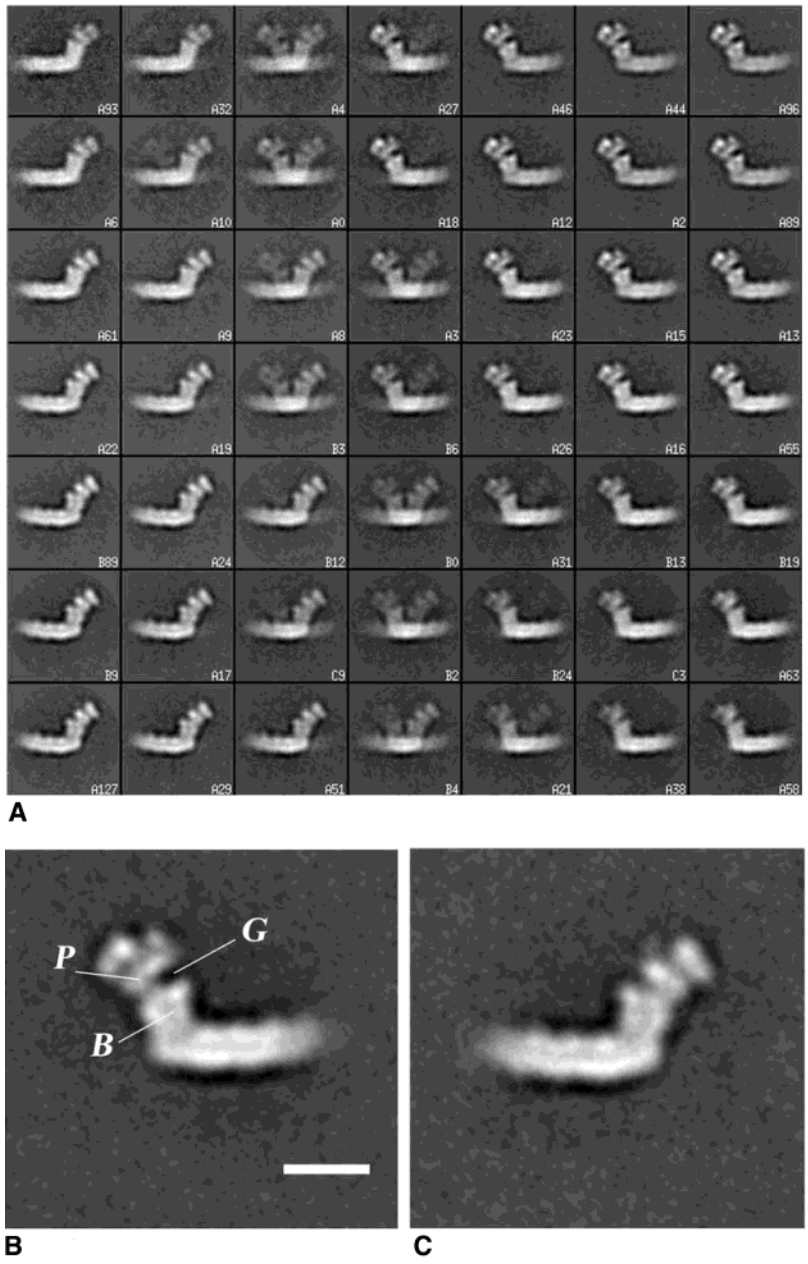

FIGURE 8: Image analysis of *A. aeolicus* complex I particles. (A) Self-organizing map from a neural network analysis of 1500 aligned particles. The numbers in the label of each square indicate the number of images that contribute to this node in the map. (B) and (C) Two averages of *A. aeolicus* complex I corresponding to a flip (B) and flop (C) position on the carbon support of the EM grid. The averages contain 815 and 685 particles, respectively (scale bar 10 nm).

doreductase from the hyperthermophilic bacterium *A. aeolicus*. Electron microscopy and single particle image analysis show two classes of averaged complex I particles, which correspond to flip and flop positions. In contrast to complex I from other species (*12*, *13*), the angle between the cytoplasmic and the membrane integrated arm of *A. aeolicus* complex I is invariant. The low-density region at the top of the vertical arm may correspond to a channel with an approximate diameter of about 1.8 nm. The low density between the peripheral and the base domain (Figure 8B) is a structural feature more pronounced in the images of the enzyme from *A. aeolicus* than from other species, although a close inspection of the images presented by Guénebaut et al. (*13*) of complex I from *E. coli* may already indicate such a feature. This finding may hint to a better preservation of the structure of the peripheral arm of the *A. aeolicus* enzyme and may indicate that complex I from *A. aeolicus* is more stable and the preparation more homogeneous than that from the other species. In this first analysis, the tip of the membrane arm, however, exhibits some blurring, and first indications exist that this blurring may be caused by variations in the length of this arm. Böttcher et al. (*39*) reported as a novel conformation a horseshoe-like shape of complex I in *E. coli* under low salt conditions. Such horseshoe-like particles were clearly not present in our preparation.

The specific activity for rotenone-sensitive reduction of ubiquinone homologous of the purified enzyme is much higher than that reported for other complex I preparations (*7*, *8*, *37*, *38*). Compared to other bacterial preparations such as that from *E. coli*, the specific activity of the highly purified *A. aeolicus* complex I is at least 29 U/mg, and a completely rotenone-sensitive activity is retained. The enzyme activity shows a biphasic decay, when exposed to high temperatures,

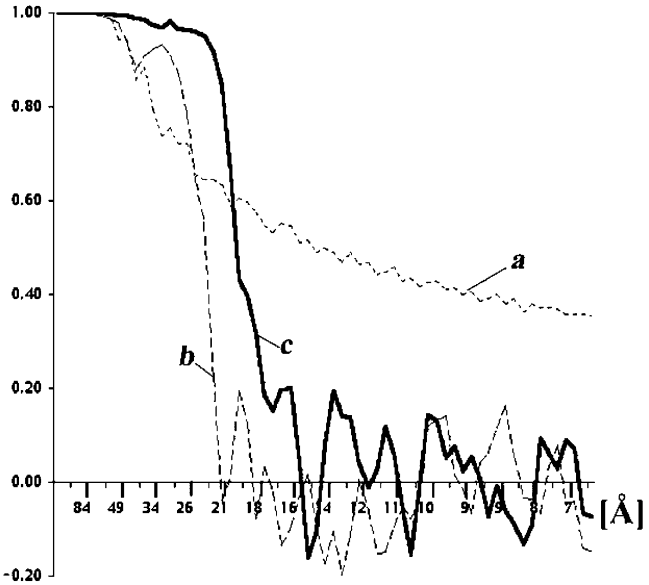

FIGURE 9: Fourier ring correlation curve of the averages shown. Because the curves for both averages were almost indistinguishable, only the curves for one average (Figure 9, curve a) are shown. With a cut off criterion of five times noise correlation (curve a), the resolution was calculated to be 2.6 nm before correction of the microscope transfer function (curve b) and 2.2 nm after correction (curve c).

with only 20% of the activity lost after 8 h at 80 °C and a half-life of 10 h. This complex I does not appear to form aggregates or to dissociate in the pH range of 4.5−7.4, with the bulk of the enzyme activity maintained at these pH extremes.

The unusual stability of the *A. aeolicus* complex I is a consequence of its adaption to high temperatures. Early work indicated increased intersubunit ion pairs and ion-pair networks in hyperthermostable enzymes (*40*). The equal increase of subclasses of oppositely charged residues in hyperthermophiles are most likely derived from the increased ion pairing at the surface of their proteins (*41*). Structural data further suggest that enhanced thermal stability involves additional features such as a higher proportion of helix forming hydrophobic residues involved in internal packing and a decreased hydrophobic surface area (*42*−*44*). Genomic sequences indicate the presence of higher levels of charged amino acids in *A. aeolicus* than in mesophilic bacteria (*21*). It is estimated that the average percentage of charged amino acids in the proteins from *A. aeolicus* is higher than 20%, and a quarter of the subunits of the *A. aeolicus* complex I contains more than 30% charged residues. A detailed structural analysis of the highly stable complex I from *A. aeolicus* may provide a system to test these assumptions for a multisubunit enzyme complex.

Thermophilic enzymes are much more rigid at room temperature than mesophilic ones, whereas both classes of enzymes show nearly identical flexibilities under their optimum working conditions (*45*). A close relationship may exist between conformational flexibility and enzyme function (*46*). This property has also been observed in the complex I preparations of *A. aeolicus*. The purified enzyme showed a detectable catalytic activity only above 50 °C and high activity under the optimal growth temperature of 85−90 °C. Similar results have been published for the membrane bound complex I (*23*). Enzymes from hyperthermophiles normally have specific activities similar to those from mesophiles (*47*). However, the specific activity of the membrane-bound complex from *A. aeolicus* appears to be at least 5-fold higher than that of a comparable preparation from *Paracoccus denitrificans*. Recent studies show that organisms living under extreme conditions adjust the lipid composition of their membranes so that a proper balance between proton permeability and the rate of outward proton pumping is maintained (*48*). However, thermophilic bacteria such as *Bacillus stearothermophilus* and *Thermotoga maritima* are prokaryotes that appear to be unable to control the proton permeability of their membranes at high growth temperatures; the membranes of these organisms were found to be very leaky to protons (*48*, *49*). We therefore suggest that the high activity of the membrane-bound complex I from *A. aeolicus* may be an adaptation to rapid proton leakage. This presumably also requires structural adaptation by *Aquifex* complex I.

Generally, the complex I in bacteria consists of 14 subunits, which have been thought to form the minimum structure of this complex (*11*). The *E. coli* complex I can be dissociated into three subcomplexes by changing pH and detergent (*7*). The subunits E, F, and G were proposed to form a NADH dehydrogenase subcomplex as a water soluble part. These three subunits in *Aquifex* complex I stick together even in the SDS-containing buffer when heated to 80 °C. This finding is indeed well-compatible with the existence of such a subcomplex. Fourteen protein bands could also be distinguished from the complex I of *A. aeolicus* by SDS−PAGE silver staining and Coomassie staining. Analysis of the genome of *A. aeolicus* reveals the presence of 24 genes homologous to complex I protein subunits from other organisms. However, they code for only 13 different nonhomologous subunits because, as mentioned before, most of them exist in two or three different versions (*21*). Therefore, different variants of complex I may be present in the isolated enzyme. However, the purified complex I always shows one band after isoelectric focusing (Figure 3B), a single sharp peak after anion exchange chromatography (data not shown), and a symmetric peak on gel filtration (Figure 2). We have identified seven subunits (Table 2), and so far, we have obtained no evidence for the existence of different variants of complex I subunits. Similar to the *E. coli* complex I (*11*, *21*), the subunits A and H−N appear to be very hydrophobic intrinsic membrane proteins, to be predicted to possess at least 63 membrane spanning segments. Variants of the other subunits present could not be decided so far because of the strongly hydrophobic nature. Further experiments are needed to identify the other individual subunits of the *Aquifex* complex I and to localize the subunits within this enzyme complex. The existence of the stable and morphologically homogeneous complex I preparation presented here will allow us to proceed in these directions.

ACKNOWLEDGMENT

We are grateful to Prof. Brian Monk for critically reading the manuscript and for helpful suggestions. We acknowledge the helpful discussions with Dr. Carola Hunte and Prof. Etana Padan during this investigation. We thank Ralf Diem for technical assistance.

REFERENCES

1. Anraku, Y. (1988) *Annu. Rev. Biochemistry 57*, 101−132.
2. Walker, J. E. (1992) *Q. Rev. Biophys. 25*, 253−324.
3. Yagi, T. (1993) *Biochim. Biophys. Acta 1141*, 1−17.
4. Spehr, V., and Schlitt, A. (1999) *Biochemistry 38*, 16261−16267.
5. Walker, J. E., Skehel, J. M., and Buchanan, S. K. (1995) *Methods Enzymol. 260*, 14−34.
6. Friedrich, T., and Steinmuller, K. (1995) *FEBS Lett. 367*, 107−111.
7. Leif, H., and Sled, V. D. (1995) *Eur. J. Biochem. 230*, 538−548.
8. Buchanan, S. K., and Walker, J. E. (1996) *Biochem. J. 318*, 243−349.
9. Kashani-Poor, N., Kerscher, S., Zickermann, V., and Brandt, U. (2001) *Biochim. Biophys. Acta 1504*, 363−370.
10. Sazanov, L. A., Burrows, P. A., and Nixon, P. J. (1998) *Proc. Natl. Acad. Sci. U.S.A. 95*, 1319−1324.
11. Friedrich, T., and Scheide, D. (2000) *FEBS Lett. 479*, 1−5.
12. Grigorieff, N. (1998) *J. Mol. Biol. 277*, 1033−1046.
13. Guénebaut, V., Schlitt, A., Weiss, H., Leonard K., and Friedrich, T. (1998) *J. Mol. Biol. 276*, 105−112.
14. Noushin, K.-P., Kerscher, S., Zickermann, V., and Brandt, U. (2001) *Biochim. Biophys. Acta 1504*, 363−370.
15. Steuber, J., Rufibach, M., and Dimroth, P. (2000) *Mol. Microbiol. 35*, 428−434.
16. Friedrich, T., Ohnishi, T., Forche, E., Kunze, B., Jansen, R., Trowitzsch, W., Hofle, G., Reichenbach, H. X., and Weiss, H. (1994) *Biochem. Soc. Trans. 22*, 226−230.
17. Brandt, U. (1999) *Biofactors 9*, 95−101.
18. Estornell, E. (2000) *Protoplasma 213*, 11−17.
19. Stetter, K. O. (1996) *FEMS Microbiol. Rev. 18*, 149−158.
20. Huber, R., Stetter, K. O. (2001) in *Bergey's manual of systematic bacteriology* (Garrity, G. M., Ed.), Vol. 1, pp 360−362, Springer-Verlag, Berlin.
21. Deckert, G., Warren, P. V., Gaasterland, T., Young, W. G., Lenox, A. L., Graham, D. E., Overbeek, R., Snead, M. A., Keller, M., Aujay, M., Huber, R., Feldman, R. A., Short, J. M., Olsen, G. J., and Swanson, R. V. (1998) *Nature 392*, 353−358.
22. Swanson, R. V. (2001) *Methods Enzymol. 330*, 158−169.
23. Scherde D., Huber R., and Friedrich T. (2002) *FEBS Lett. 512*, 80−84.
24. Laemmli, U. K. (1970) *Nature 227*, 680−766.
25. Schägger, H. (1994) in *A practical guide to membrane protein purification* (von Jagow, G., and Schägger, H., Eds.) pp 59−79, Academic Press, Inc., San Diego.
26. Estornell E., Fato, R., Pallotti, F., and Lenaz, G. (1993) *FEBS Lett. 332*, 127−131.
27. Stoops, J. K., Kolodziej, S. J., Schroeter, J. P., Bretaudiere, J. P., and Wakil, S. J. (1992) *Proc. Natl. Acad. Sci. U.S.A. 89*, 6585−6589.
28. Frank, J., Radermacher, M., Penzcek, P., Zhu, J., Li, Y., Ladjadj, M., and Leith, A. (1996) *J. Struct. Biol. 116*, 190−199.
29. Marabini, R., Masegosa, I. M., San Martin, M. C., Marco, S., Fernandez, J. J., de la Fraga, L. G., Vaquerizo, C., and Carazo, J. M. (1996) *J. Struct. Biol. 116*, 237−240.
30. Radermacher, M., Ruiz, T., Wieczorek, H., and Gruber, G. (2001) *J. Struct. Biol. 135*, 26−37.
31. Marabini, R., and Carazo, J. M. (1994) *Biophys. J. 66* (6), 1804−1814.
32. Saxton, W. O., and Baumeister, W. (1982) *J. Microsc. 127*, 127−138.
33. Hunte, C., Koepke, J., Lange, C., Rossmanith, T., and Michel, H. (2000) *Struct. Fold. Des. 8* (6), 669−684.
34. Krogh, A., Larsson, B., von Heijne, G., and Sonnhammer, E. L. L. (2001) *J. Mol. Biol. 305*, 567−580.
35. Sonnhammer, E. L. L., von Heijne, G., and Krogh, A. (1998) in *Proceedings of the Sixth International Conference on Intelligent Systems for Molecular Biology* (Glasgow, J., Littlejohn, T., Major, F., Lathrop, R., Sankoff, D., and Sensen, C., Eds.) pp 175−182, AAA1 Press, Menlo Park, CA.
36. Schults, U., Haupt, V., Abelmann, A., Fecke, W., Brors, B., Rasmussen, T., Friedrich, T., and Weiss, H. (1999) *J. Mol. Biol. 292*, 569−580.
37. Okun, J. G., Zickermann, V., Zwicker, K., Schägger, H., and Brandt, U. (2000) *Biochim. Biophys. Acta 1459*, 77−87.
38. Yagi, T. (1986) *Arch. Biochem. Biophys. 250*, 302−311.
39. Böttcher, B., Scheide D., Hesterberg, M., Nagel-Steger, L., and Friedrich, T. (2002) *J. Biol. Chem. 277* (20) 17970−17977.
40. Perutz, M. F., and Raidt, H. (1975) *Nature 255*, 256−259.
41. Cambillau, C., and Claverie, J. M. (2000) *J. Biol. Chem. 275*, 32383−32386.
42. Danson, M. J., and Hough, D. W. (1997) *Comp. Biochem. Phys. 117*, 307−312.
43. Hough, D. W., and Danson, M. J. (1999) *Curr. Opin. Chem. Biol. 3*, 39−46.
44. Argos, P., Rossmann, M. G., Grau, U. M., Zuber, H., Frank, G., and Rratschin, J. D. (1979) *Biochemistry 18*, 5698−5703.
45. Zavodszky, P., Kardos, J., Svingor A. G. A., and Petsko, P. (1998) *Proc. Natl. Acad. Sci. U.S.A. 95*, 7406−7411.
46. Svingor, A., Kardos, J., Hajdu, I., Nemeth, A., and Zavodszky, P. (2001) *J. Biol. Chem. 276*, 28121−28125.
47. Daniel, R. M., and Danson, M. J. (2001) *Methods Enzymol. 330*, 283−293.
48. Albers, S. V., van de Vossenberg, J. L. C. M., Driessen, A. J. M., and Konings, W. N. (2000) *Front. Biosci. 5*, 796−803.
49. van de Vossenberg, J. L. C. M., Ubbink-Kok, T., Elferink, M. G. L., Driessen, A. J. M., and Konings, W. N. (1995) *Mol. Microbiol. 18*, 925−932.

BI026876V